7570–7580 Nucleic Acids Research, 2009, Vol. 37, No. 22 Published online 9 October 2009
doi:10.1093/nar/gkp840

Stabilization of G-quadruplex in the *BCL2* promoter region in double-stranded DNA by invading short PNAs

Mykola I. Onyshchenko[1], Timur I. Gaynutdinov[1], Ethan A. Englund[2], Daniel H. Appella[2], Ronald D. Neumann[1] and Igor G. Panyutin[1,*]

[1]Department of Radiology and Imaging Sciences, Clinical Center and [2]Laboratory of Bioorganic Chemistry, NIDDK, National Institutes of Health, Bethesda, MD 20892, USA

Received July 29, 2009; Revised September 18, 2009; Accepted September 21, 2009

ABSTRACT

Numerous regulatory genes have G-rich regions that can potentially form quadruplex structures, possibly playing a role in transcription regulation. We studied a G-rich sequence in the *BCL2* gene 176-bp upstream of the P1 promoter for G-quadruplex formation. Using circular dichroism (CD), thermal denaturation and dimethyl sulfate (DMS) footprinting, we found that a single-stranded oligonucleotide with the sequence of the *BCL2* G-rich region forms a potassium-stabilized G-quadruplex. To study G-quadruplex formation in double-stranded DNA, the G-rich sequence of the *BCL2* gene was inserted into plasmid DNA. We found that a G-quadruplex did not form in the insert at physiological conditions. To induce G-quadruplex formation, we used short peptide nucleic acids (PNAs) that bind to the complementary C-rich strand. We examined both short duplex-forming PNAs, complementary to the central part of the *BCL2* gene, and triplex-forming bis-PNAs, complementary to sequences adjacent to the G-rich *BCL2* region. Using a DMS protection assay, we demonstrated G-quadruplex formation within the G-rich sequence from the promoter region of the human *BCL2* gene in plasmid DNA. Our results show that molecules binding the complementary C-strand facilitate G-quadruplex formation and introduce a new mode of PNA-mediated sequence-specific targeting.

INTRODUCTION

The *BCL2* gene, named after B-cell lymphoma 2, encodes an apoptosis inhibitor protein. BCL2 protein is localized on the mitochondrial membrane and helps maintain the delicate balance between programmed cell death and survival. Due to its role in apoptosis regulation, the *BCL2* gene is an important target in anticancer treatment using pro-apoptotic drugs. Increased levels of *BCL2* mRNA are found in many human cancers, such as B- and T-cell lymphomas (1), breast (2), cervical (3), lung (4) and prostate/colorectal cancers (5). Thus, the *BCL2* gene is included in the proto-oncogene family as a potent factor inhibiting apoptosis (6). Furthermore, insufficient expression of the *BCL2* gene may lead to increased apoptotic activity in cells resulting in various degenerative diseases such as multiple sclerosis (7), Alzheimer's disease (8), Parkinson's disease (9), stroke (10) and spinal cord injuries (11).

The human *BCL2* gene has two promoters, P1 and P2 (12). P1, the major promoter, is located 1.3- to 1.5-kbp upstream of the translation start site (spanning from −3934 to −1280 bp). Although it has a few TATA regions, the P1 promoter is mainly GC rich, with numerous transcription initiation sites. The P2 promoter has multiple TATA regions and is located 1.3-kbp downstream of P1. Recently, another promoter (designated as M) was discovered in the region between P1 and P2 sites. Promoter M acts in a p53-dependent manner and has suppressive activity on P1 and P2 promoters (13). P2 and M promoters apparently modulate P1 activity, while P1 appears to be the main driving force regulating *BCL2* transcription.

Hurley *et al.* (14, 15) describe the formation of quadruplex structures in a GC-rich region located −58 to −19 bp upstream of the *BCL2* P1 promoter (indicated on Figure 1 as *bcl2G4-1*). Multiple transcription factors bind to this region, which suggests its importance for P1 promoter regulation (16–18). For our study, we selected another G-rich sequence from the *BCL2* gene promoter located 176-bp upstream of P1 promoter that exhibited G-quadruplex forming potential. We refer to this sequence as *bcl2G4-2* (Figure 1).

*To whom correspondence should be addressed. Tel: +1 301 496 8308; Fax: +1 301 480 9712; Email: igorp@helix.nih.gov

Guanine-rich sequences with quadruplex forming potential are located in the promoter regions of numerous genes, especially regulatory genes (19). Quadruplex formation has been examined in several genes such as *PDGF-A* (20,21), *VEGF* (21–23), c-*myc* (21,24), *KRAS* (25), *BCL2* (14,15). In most cases, G-quadruplex formation was studied in single-stranded DNA (ssDNA) oligonucleotides under various conditions *in vitro*. Data on G-quadruplex formation in double-stranded (ds) plasmids are rare, likely reflecting a lower potential for these structures to form under supercoiling stress conditions compared with other non-B DNA conformations such as Z-DNA or H-DNA triplex (26,27). One of the first examples of quadruplex formation in plasmids was observed by electron microscopy. The authors developed a plasmid with guanine-rich inserts and observed a 'G-loop' DNA/RNA hybrid on the C-rich strand and a G-quadruplex on the complimentary strand. They concluded that the RNA/DNA hybrid was critical for G-quadruplex stabilization in the post-transcriptional G-loops (28).

In this article, we report the formation of G-quadruplexes in ds plasmid DNA when peptide nucleic acids (PNAs) bind to the complementary C-strand. PNAs are nucleic acid mimics with the canonical nucleobases connected to an achiral, uncharged polyamide backbone (29,30). PNA forms very stable duplexes and triplexes with complementary DNA, displacing the complementary DNA strand in DNA duplexes and producing so-called PD-loops (31–33). We designed short duplex- and triplex-forming PNAs that are able to invade dsDNA of the *BCL2* gene by selectively binding to the complementary cytosine-rich sequence, thus promoting quadruplex formation in the guanine-rich segments. Because the anticipated quadruplex would be solely DNA, this approach differs from strategies targeting G-rich sequences by forming PNA/DNA hybrid quadruplexes (34–36).

Initially, we examined the G-quadruplex forming potential of a single-stranded sequence from the guanine-rich region of the *BCL2* gene (*bcl2G4-2*) *in vitro*. We then inserted the *bcl2G4-2* sequence into plasmid DNA and studied whether quadruplexes could form in the G-rich strand of dsDNA in different conditions. Specifically, we employed several types of PNA oligomers and the quadruplex-stabilizing drug telomestatin. Our results show that PNA binding to the complementary C-strand is required for the G-quadruplex formation in the G-rich strand and suggest a new mode of sequence-specific targeting.

MATERIALS AND METHODS

DNA oligonucleotides

The DNA oligonucleotides (Table 1) were synthesized on an ABI394 DNA synthesizer (PE Applied Biosystems, Foster City, CA, USA), and purified by denaturing polyacrylamide gel electrophoresis (PAGE) as described previously (37). The absorbance of single-stranded oligonucleotide solutions were measured at 260 nm on an HP 8452A Diode Array Spectrophotometer, and the concentrations were calculated with extinction coefficient calculator software (http://www.basic.northwestern.edu/biotools/oligocalc.html). Several guanosines in *BCL2doublePPG* (marked as P) were substituted with 8-aza-7-deaza-2′-deoxyguanosine (PPG) (38). Partially duplex DNA oligonucleotides were obtained by annealing of complementary strands by slow cooling from 95°C to room temperature. The DNA oligonucleotides were incubated in 20 mM Tris–HCl buffer solution (pH 7.4) at 37°C for 1 h and in the presence or absence of 100 mM NaCl or 100 mM KCl.

PNAs

Bis-PNAs were purchased from Panagene, South Korea. Central-binding PNAs (two short G-rich sequences) were synthesized via Boc-mediated solid phase synthesis on a 433A Automated Peptide Synthesizer from Applied Biosystems (39). Boc-protected PNA monomers were purchased from PE Applied Biosystems. PNA oligomer quality was tested using an HP 1050 high performance liquid chromatography (HPLC) and spectrophotometrically (HP 8452A Diode Array Spectrophotometer). PNA concentration was measured at 260 nm on an HP 8452A Diode Array Spectrophotometer, and was calculated with extinction coefficient calculator software (http://www.basic.northwestern.edu/biotools/oligocalc.html). Prior to all experiments, PNAs were incubated in a shaker for 15 min at 42°C and their concentration was measured before mixing with DNA samples. PNA sequences are presented in Table 2.

Plasmids

Plasmids carrying the appropriate inserts were obtained by cloning of the *BCL2single* oligonucleotide (the same G-rich sequence with short TTCCTTT regions for triplex formation with bis-PNAs) with the corresponding complementary strand into pCR-Blunt vector using the Zero Blunt PCR Cloning Kit (Invitrogen, Carlsbad, CA, USA). Constructs were incorporated and amplified using the One Shot TOP10 Chemically Competent *Escherichia coli* (Invitrogen) and selected with 50 μg/ml kanamycin. Plasmid DNA was purified using the Plasmid Maxi Kit (Qiagen, Valencia, CA, USA). All procedures were performed according to the manufacturer's recommendations. Plasmids were additionally purified by ultracentrifugation in a CsCl gradient (40). All plasmids were sequenced to confirm the desired insertion using the Maxam–Gilbert sequencing procedure (41). Incubation of plasmids with PNAs was performed in 20 mM potassium acetate (pH 5.2) with or without 10 μM telomestatin at 37°C overnight with molar ratio 100:1 PNA to DNA.

Dimethyl sulfate footprinting of oligonucleotides

DNA oligonucleotides were 5′-^{32}P-labeled with [γ-^{32}P]-ATP (Perkin Elmer, Waltham, MA, USA) by T4 polynucleotide kinase using standard protocol followed by purification on G-25 microcolumns (GE Healthcare, UK). After incubation under various conditions, samples were probed with 2 μl 10% dimethyl sulfate (DMS) in ethanol for 15 min at 15°C. The reaction was terminated

with stop solution on ice (1.5 M sodium acetate, pH 5.2, 1 M β-mercaptoethanol, 100 μg/ml yeast tRNA) followed by ethanol precipitation and washing with 70% ethanol. After incubation in 10% piperdine at 95°C for 20 min and repeated lyophilizations, samples were analyzed by electrophoresis in 12% denaturing polyacrylamide gels. Gels were quantified using BAS-2500 Bioimager (FUJI Medical Systems USA, Stamford, CT, USA). To measure the intensity of the individual bands, the intensity profile of each lane was generated from the digitized gel image using Image Gauge software (FUJI Medical Systems USA). Band intensities were normalized with control samples (Tris–HCl buffer), inverse values are presented.

Thermal denaturation spectrophotometry

Absorbance spectra measurements were performed on an HP 8452A Diode Array Spectrophotometer. DNA oligonucleotides were placed in quartz cuvettes with an optical path length of 1 cm. Absorbance spectra were recorded in 220–335 nm range from 90°C to 20°C during slow cooling down of the samples (0.5°C per min) in the presence of 100 mM KCl in 20 mM Tris–HCl buffer solution (pH 7.4). Spectra at 90°C were subtracted from those at 20°C and normalized on oligonucleotide concentration. The temperature-dependant absorbance at 295 nm was also recorded.

Circular dichroism spectroscopy

Circular dichroism (CD) spectra measurements were performed on Jasco J-810 spectrophotometer in a 2-mm path length cuvette and a wavelength scanning speed of 100 nm/min. DNA oligonucleotides were incubated for G-quadruplex formation as described above. CD spectra of samples in the presence of 100 mM KCl and 20 mM Tris–HCl (pH 7.4) were measured at 20°C in the range from 200 nM to 320 nM. The spectra (the averages of three scans) were corrected on blank buffer spectra and normalized on oligonucleotide concentration.

Chemical probing of plasmid DNA

Plasmid DNA samples contained 1 μg of plasmid in 40 mM TE buffer (pH 7.4) with or without 100 mM KCl and 100 mM NaCl or 20 mM potassium acetate (pH 5.2). Plasmids incubated with PNAs were chemically modified to a total volume of 50 μl with 2.5 mM OsO_4 plus 2.5 mM 2.2′-dipyridyl disulfide for 5 min at room temperature, with 2 μl diethylpyrocarbonate (DEPC) for 5 min at room temperature, or with 2 μl 10% DMS in ethanol for 15 min at 15°C. Reactions were terminated with stop solution on ice (1.5 M sodium acetate, pH 5.2, 1 M β-mercaptoethanol and 100 μg/ml yeast tRNA) followed by ethanol precipitation and washing with 70% ethanol. Modified plasmids were cut by incubation with Fast Digest SpeI and Kpn1 restriction enzymes (Fermentas, Hanover, MD, USA) for 1 h at 37°C followed by 3′-^{32}P-labeling with [α-^{32}P]-dCTP (Perkin Elmer) by Klenow fragment of DNA polymerase I (Fermentas). After purification on G-50 microcolumns (GE Healthcare) followed by incubation in 10% piperidine at 95°C for 20 min and repeated lyophilizations, samples were analyzed by electrophoresis on 12% denaturing polyacrylamide gels without fragment purification, allowing the shorter fragment to run off the gel. For DMS protection analysis, intensities of bands corresponding to guanines were measured and normalized on that of guanines outside G-rich sequence.

RESULTS

Formation of G-quadruplex structures by G-rich strands of *BCL2* gene

To test the possibility of G-quadruplex formation in the *BCL2* guanine-rich sequence, we synthesized ssDNA with the sequences from the region of *BCL2* 176-bp upstream of the P1 promoter (*bcl2G4-2*, Figure 1). The guanine-rich region *bcl2G4-2* was adjacent to a short ds portion of the molecule to better mimic conditions in a plasmid and to prevent single-strand tail interaction, possibly affecting quadruplex formation (42). The resulting *BCL2double* is a partially ds oligonucleotide with a single-stranded G-rich region with seven guanine runs (Table 1). For a positive control, *T2G4double* oligonucleotide was synthesized, which has a ds part similar to *BCL2double* and a single-stranded G-rich region from *Tetrahymena thermophila* telomeres. For a negative control, we synthesized an oligomer containing multiple PPG

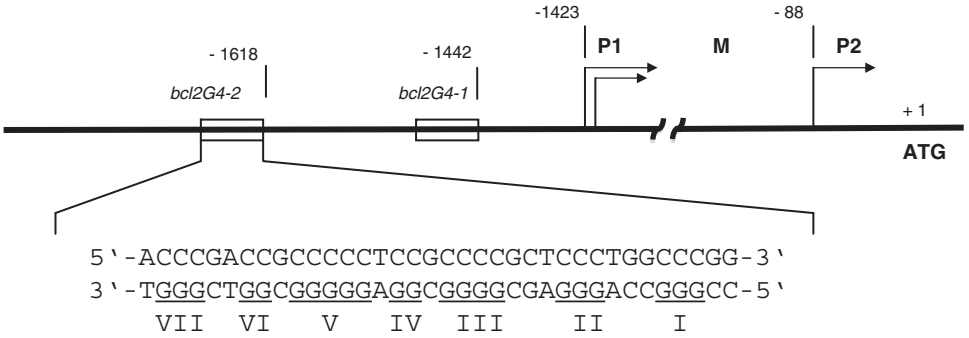

Figure 1. Promoter structure of the human *BCL2* gene; shown *bcl2G4-2* insert is a 51-mer sequence of guanine-rich strand. Runs of guanines are underlined and marked.

Table 1. Sequences of DNA oligonucleotides used in the study

Name	Sequence
BCL2single	5′-TTTCCTTCCGGGCCAGGGAGCGGGGCGGAGGGGGCGGTCGGGTGTTTCCTT-3′ I II III IV V VI VII
BCL2double	5′-GAGAACAGTCAACATACAGTGTTAGGGCCAGGGAGCGGGGCGGAGGGGGCGGTCGGGT-3′ 3′-CTCTTGTCAGTTGTATGTCACAAT-5′
BCL2doublePPG	5′-GAGAACAGTCAACATACAGTGTTAGGGCCAGGGAGCGGPPCGGAGGGPPCGGTCGPPT-3′ 3′-CTCTTGTCAGTTGTATGTCACAAT-5′
T2G4double	5′-GAGAACAGTCAACATACAGTGTTAGGGGTTGGGGTTGGGGTTGGGGCGGTCGGGT-3′ 3′-CTCTTGTCAGTTGTATGTCACAAT-5′

P = 8-aza-7-deaza-2′-deoxyguanosine (PPG).

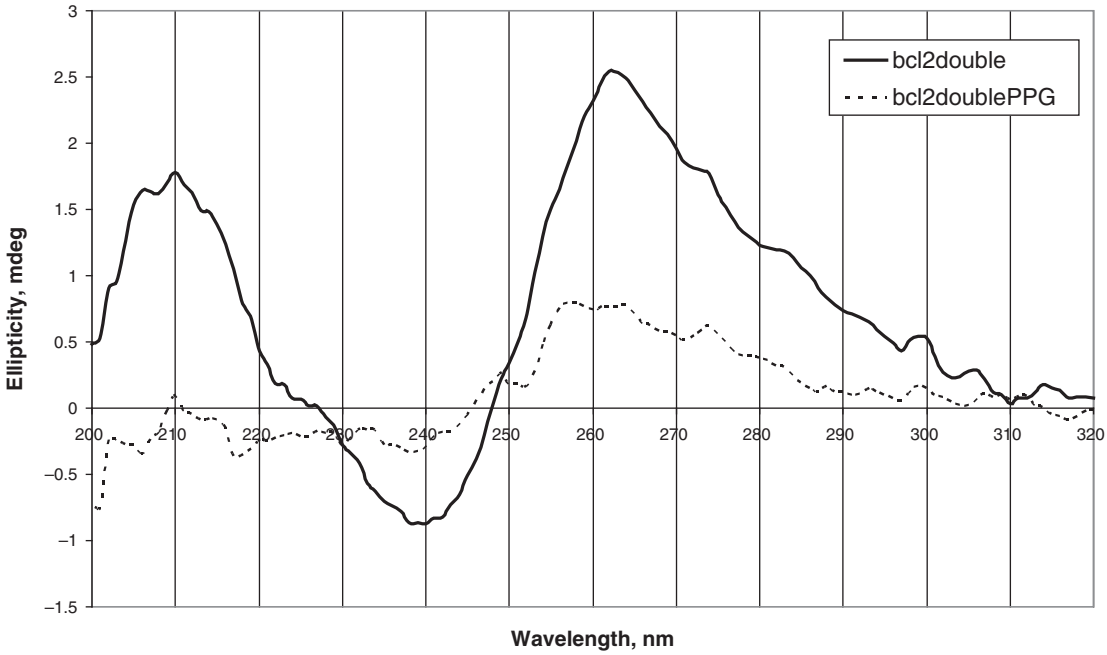

Figure 2. CD spectral analysis of *BCL2double* (solid line) and *BCL2doublePPG* (dash line). CD spectra of the samples in the presence of 100 mM KCl and 20 mM Tris–HCl (pH 7.4) were measured at 20°C in the range from 200 nM to 320 nM. The spectra (the averages of three scans) were corrected on blank buffer spectrum and normalized on oligonucleotide concentration.

nucleoside units (*BCL2doublePPG*). The PPG guanine analog lacks N7 nitrogen, eliminating the possibility of hydrogen bonding to the Hoogsteen face, thus precluding quadruplex formation (38). Oligonucleotide sequences are presented in Table 1. Runs of guanines are marked with roman numerals from I to VII; PPGs are marked as 'P'.

CD spectroscopy

CD spectroscopy studies were performed to obtain evidence for the presence of G-quadruplex structures in the *BCL2* sequence. CD spectroscopy has been widely used for the characterization of G-quadruplex-forming oligonucleotides (43,44). We acquired CD spectra of *BCL2double* and *BCL2doublePPG* in 100 mM KCl and 20 mM Tris–HCl buffer (pH 7.4) at 20°C. DNA oligonucleotides were incubated for G-quadruplex formation in the buffer solution at 37°C for 1 h. Data are shown in Figure 2. The solid line represents the CD spectrum of *BCL2double*, while a dashed line represents the control, *BCL2doublePPG*. The *BCL2double* CD spectrum has a prominent positive peak at ~260 nm and a negative peak at 240 nm. However, the CD spectrum of *BCL2doublePPG* is almost flat, lacking distinguishable maxima or minima. The lack of ellipticity evidenced in *BCL2doublePPG* can be attributed to the lack of N7 nitrogen hydrogen bonding capabilities, eliminating the possibility of quadruplex formation. CD spectra are generally affected by the orientation of guanine residues relative to the sugar moieties, so that parallel and antiparallel quadruplexes can be distinguished. Based on the spectra of short G-rich telomeric oligonucleotides that form tetramolecular parallel structures, the positive peak near 260 nm and negative peak near 240 nm are characteristic for the parallel G-quadruplex conformation (45–47). Based on these data, the *BCL2double* sequence forms G-quadruplexes in the presence of potassium ions with a CD spectrum resembling that of parallel quadruplex.

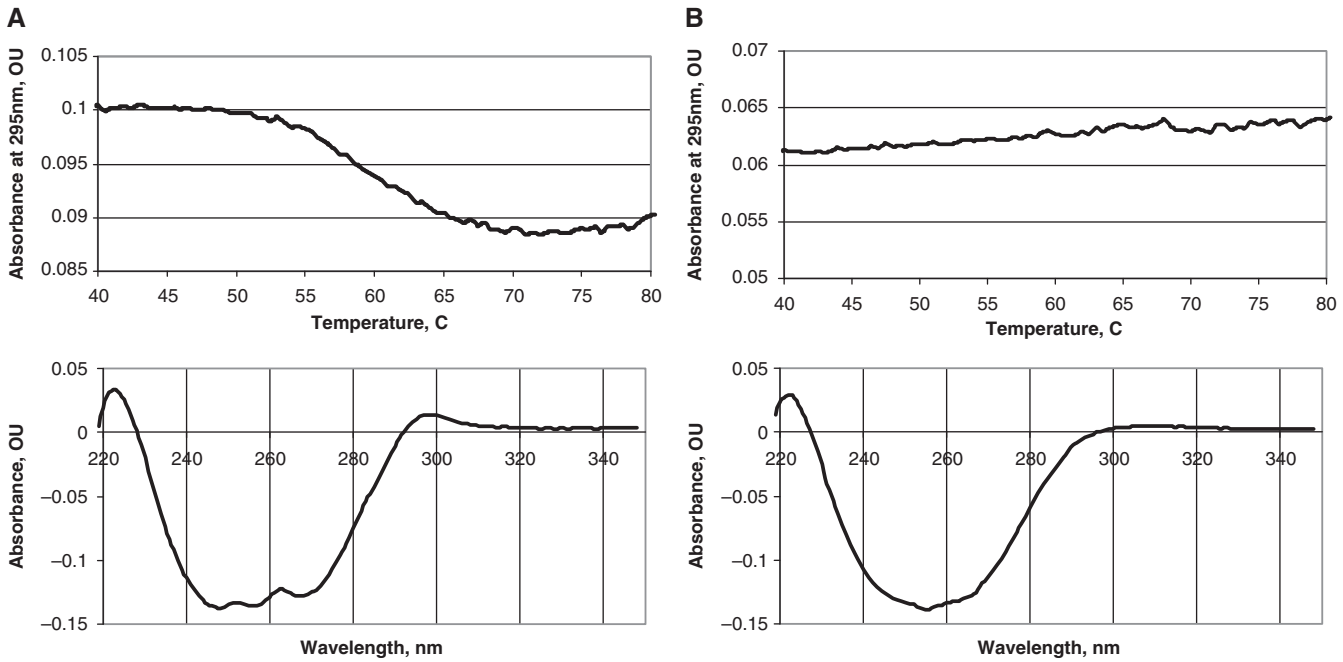

Figure 3. Thermal denaturing spectral absorbance analysis of *BCL2double* (**A**) and *BCL2doublePPG* (**B**). Absorbance spectra were recorded in 220–335 nm range from 90°C to 20°C during slow cooling of the samples (0.5°C per min) in the presence of 100 mM KCl in 20 mM Tris–HCl buffer solution (pH 7.4). Upper panels: absorbance at 295 nm depending on temperature; lower panels: spectra at 90°C were subtracted from those at 20°C and normalized on oligonucleotide concentration.

Thermal denaturation

Further spectroscopic evidence for the presence of G-quadruplex structures in the *BCL2* promoter region was obtained from annealing studies of *BCL2double* and *BCL2doublePPG*. Absorbance spectra were recorded in 220–335 nm range at 20°C and 90°C during slow cooling of the samples (0.5°C per min) in the presence of 100 mM KCl in 20 mM Tris–HCl buffer solution (pH 7.4). Figure 3A shows data for *BCL2double*, and Figure 3B for *BCL2doublePPG*. The renaturation curve at 295 nm reveals a transition with melting temperature (T_m) of ~60°C (Figure 3A, upper panel) for *BCL2double*. No melting transition was evident for *BCL2doublePPG*. Spectra at 90°C were subtracted from those at 20°C and normalized on oligonucleotide concentration. It was previously described that differential absorbance spectra of G-quadruplex structures have a characteristic peak in absorbance at 295 nm (48). This peak is observed in the case of *BCL2double* along with the expected negative peak for oligonucleotides at 260 nm (Figure 3A, bottom panel). However, the differential spectrum of *BCL2doublePPG* lacks the peak at 295 nm (Figure 3B, bottom panel). Thus, thermal denaturation studies support G-quadruplex formation in the *BCL2double* sequence in potassium-containing buffer.

Chemical probing

For further evidence of G-quadruplex formation, we probed *BCL2double* and *T2G4double* with DMS (see 'Materials and Methods' section). This assay detects guanines in a G-quadruplex due to protection of their N7 positions from DMS modification. Samples were probed in 100 mM KCl, 20 mM Tris–HCl buffer solution (pH 7.4) and analyzed in 12% denaturing PAGE (Figure 4, right panel). The intensity of the individual bands in gels was measured and normalized to control samples probed with DMS in the same Tris–HCl buffer without KCl. The inverse values are presented on the graph (Figure 4). Both oligonucleotides tend to form G-quadruplex structures in the presence of potassium ions after incubation at 37°C for 1 h. DMS protection is observed in the range of 60–90% (quantified for *BCL2double*) depending on the position of guanines along the sequence. Guanines with a higher degree of protection that apparently participate in G-quadruplex formation are marked with asterisks. They correspond to the G-runs II, III, V and VI. Incubation of *BCL2double* and *T2G4double* in 100 mM NaCl at 37°C for 1 h resulted in strong DMS protection of guanines in *T2G4double* and very weak DMS protection in the case of *BCL2double* (very close to control without NaCl). These results suggest that *T2G4double* forms G-quadruplex structures in the presence of both potassium and sodium ions (Supplementary Figure S1), while *BCL2double* formed quadruplexes only in the presence of potassium.

G-quadruplex formation in plasmids

After showing evidence that the G-rich sequence of the *BCL2* promoter has the potential to form G-quadruplexes in single-stranded oligonucleotides, we extended our studies of these structures to ds plasmid DNA. We used several chemical probes to quantify local dsDNA melting

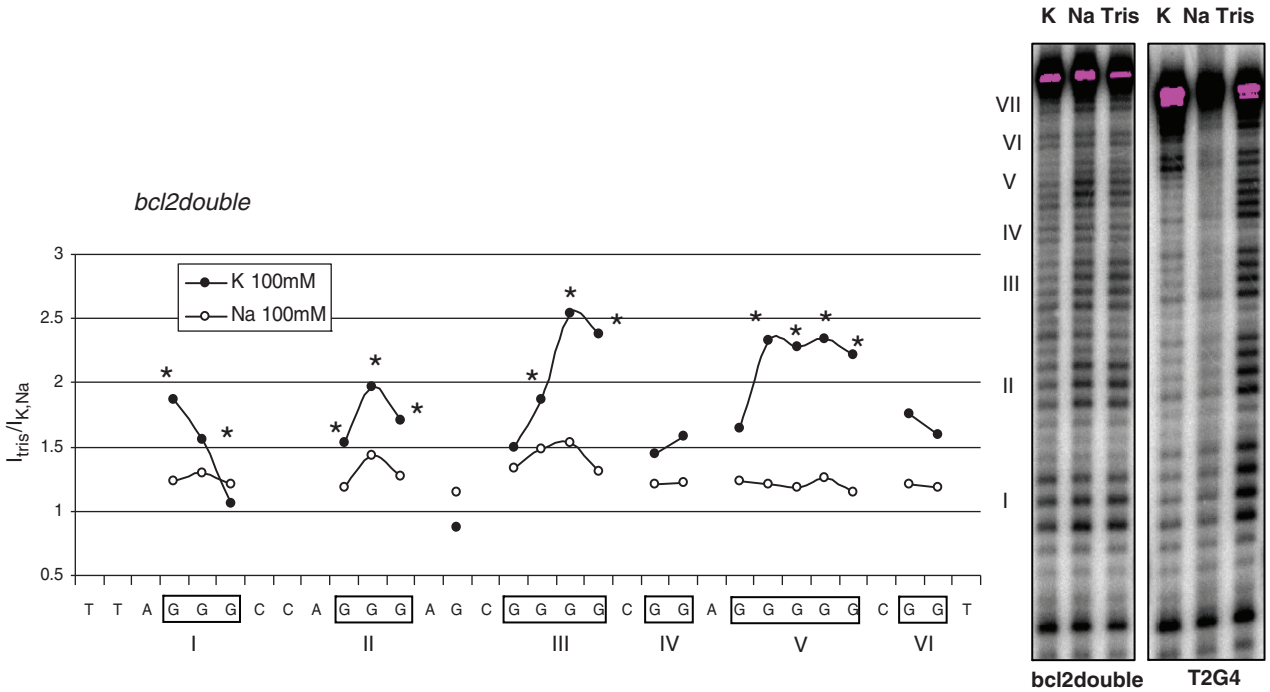

Figure 4. DMS footprinting of *BCL2double* and *T2G4double*. Samples were incubated in the presence or absence of 100 mM NaCl (open circles) and 100 mM KCl (closed circles) in 20 mM Tris–HCl buffer solution (pH 7.4) at 37°C for 1 h and then probed with 2 µl 10% DMS in ethanol for 15 min at 15°C. For quantification, band intensities were normalized with control samples (20 mM Tris–HCl buffer alone), and inverse values are presented on graphs to the left. Guanines marked with asterisk are the most protected. Guanine runs are marked with roman numerals (I–VII).

at the desired location. First, we probed DNA with OsO_4 and DEPC, allowing us to determine if thymines and adenines, respectively, are open within the insert. Second, we used DMS probing to reveal quadruplex formation from the protection at the N7 position. We used plasmid samples with natural superhelical density. Samples were incubated in the presence or absence of 100 mM KCl, 100 mM NaCl and 10 µM telomestatin for 1 h at 37°C. Probing with DEPC and OsO_4 did not show local melting in the insert region (Supplementary Figure S2). Overall, we were not able to detect any evidence of stable local DNA melting or G-quadruplex formation within the insert in the presence of potassium, sodium or telomestatin.

G-quadruplex formation in plasmids incubated with PNA

Because local melting conditions likely contribute to the quadruplex formation in plasmid DNA, PNA probes were designed and synthesized to selectively bind the cytosine-rich complementary strand of the guanine-rich *BCL2* sequence. Two PNA designs were employed: bis-PNAs that form triplexes with DNA regions bordering the guanine-rich region and central-binding PNAs (cPNAs) that form duplexes to the complementary cytosine-rich strand directly across from the quadruplex forming region. The PNAs used are presented in Table 2, and the concept is depicted in Figure 5. Since triplex-forming PNAs require a polypurine–polypyrimidine sequence, we added TTTCCTT regions to both ends of the G-rich sequence (*BCL2single*, Table 1). Incubation of plasmids

Table 2. Sequences of PNA oligonucleotides used in the study

Name	Sequence
Bis-PNA (openers)	(Lys)2-TTJ-JTT-T-(eg1)$_3$-TTT-CCT-T-NH_2
cPNA1	Lys-GGGCGGAGG-NH_2
cPNA2	Lys-GCCAGGGA-NH_2

eg1 = 8-amino-3,6-dioxaoctanoic acid linker.

with or without PNAs and with or without telomestatin was performed in 20 mM potassium acetate (pH 5.2) at 37°C overnight with molar ratio 100:1 PNA to DNA. Low pH buffer was used because protonated cytosines are required for stable triplex formation. Figure 6 represents the results of probing the plasmid DNA with a *BCL2single* insert with OsO_4, DEPC and DMS. Only the G-rich strand was analyzed. Samples were probed in 20 mM KOAc, pH 5.2. Probing procedures were the same as in the previous step of the experiment. Control samples were incubated only in KOAc buffer (lanes 1, 7 and 13). Experimental samples were incubated with bis-PNAs (lanes 3, 9 and 15), central-binding PNAs (lanes 2, 8 and 14), both PNA types (lanes 4, 10 and 16), both PNA types with 10 µM telomestatin (lanes 5, 11 and 17) and only 10 µM telomestatin (lanes 6, 12 and 18). Lanes 1–6, 7–12 and 13–18 show probing with OsO_4, DEPC and DMS, respectively. Results suggest stable binding of bis-PNAs and central-binding PNAs to naturally supercoiled plasmid DNA. Data in Figure 6 clearly demonstrate

local melting of the targeted DNA region with opening of the G-rich strand. OsO_4 modifications of thymines in lanes 3, 4 and 5 correspond to binding of bis-PNA openers to the complementary C-rich strand, while OsO_4 modification of thymines in lanes 2, 4 and 5 correspond to binding of cPNAs to the central part of the complementary strand within the insert. Lanes 8, 10 and 11 reveal opening of adenines as a result of cPNA invasion and binding to the complementary strand of the insert. The highest yield of modification was observed with a combination of both bis-PNA openers and central-binding PNAs with and without telomestatin (lanes 4, 5, 10 and 11 in Figure 6).

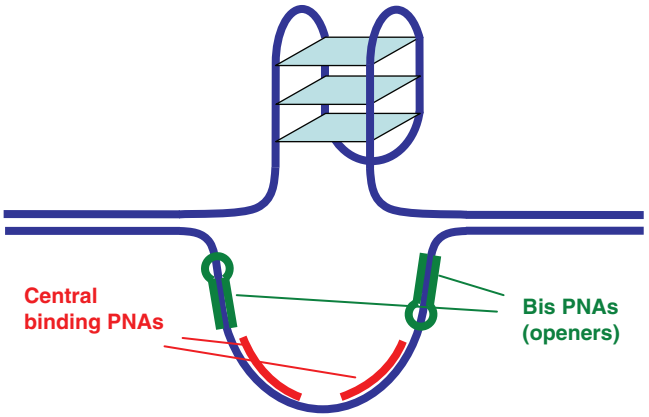

Figure 5. Proposed design for PNA binding to G-rich DNA region.

Next, we tested for G-quadruplex formation using a DMS protection assay. We measured the intensity of the individual bands after DMS probing (lanes 12–18) and normalized to guanines outside the G-rich sequence. Guanine protection from DMS was observed in all experimental lanes (lanes 14–17 in Figure 6) except for the sample incubated with only telomestatin (lane 18). The panel on the left in Figure 6 represents quantified data for DMS protection assay. Incubation with telomestatin alone did not lead to DMS protection; on the contrary, guanines were modified at a slightly higher rate. Samples incubated with PNAs showed a significant protection from DMS methylation. The most effective protection appeared to be in the case of incubation with

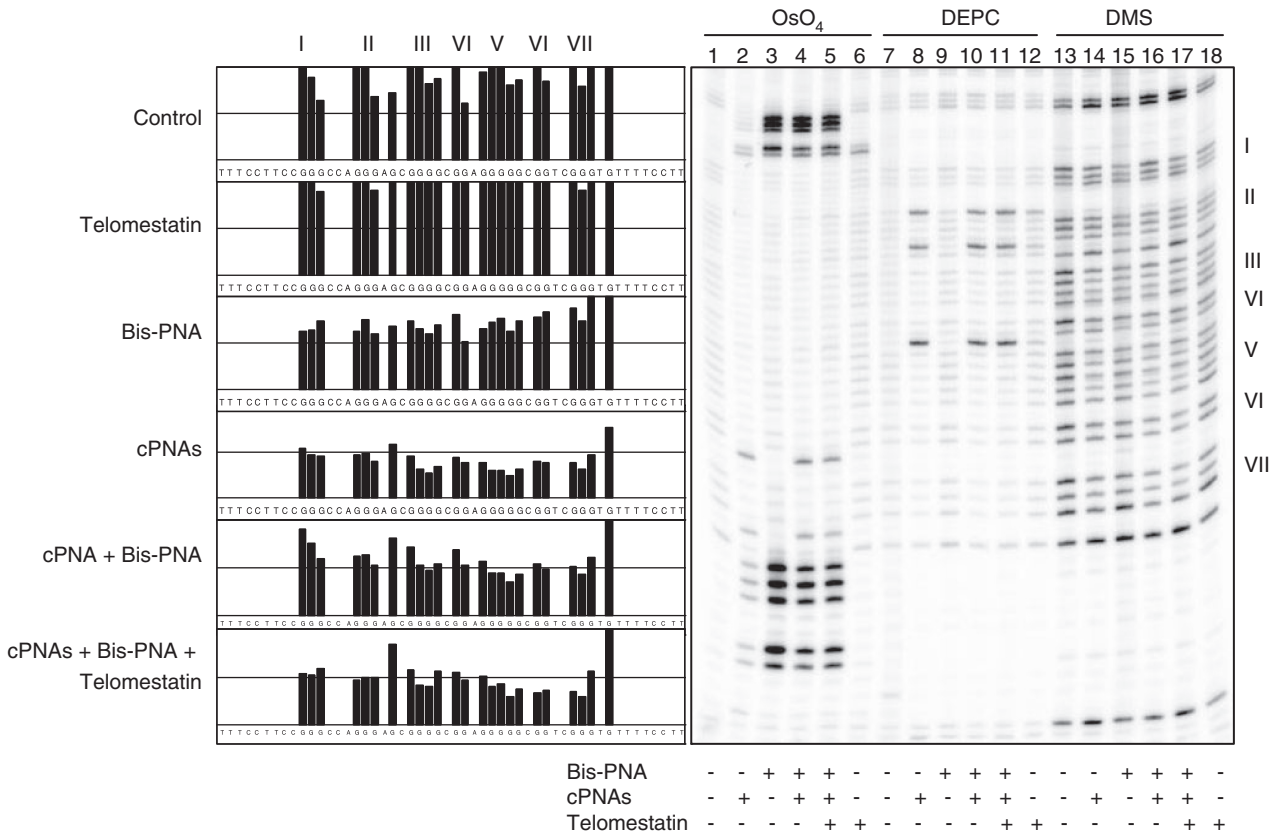

Figure 6. PNA binding studies. Chemical probing of plasmid with *BCL2* insert with PNAs. Incubation of plasmids with PNAs was performed in 20 mM potassium acetate (pH 5.2) at 37°C overnight with molar ratio 100:1 PNA to DNA. Control sample was incubated only in potassium acetate buffer (lanes 1, 7 and 13). Experimental samples were incubated with bis-PNA (lanes 3, 9 and 15), central-binding PNAs (lanes 2, 8 and 14), with both PNA types without 10 μM telomestatin (lanes 4, 10 and 16), with both PNA types with telomestatin (lanes 5, 11 and 17) and only with 10 μM telomestatin (lanes 6, 12 and 18). Samples containing 1 μg of plasmid in 20 mM potassium acetate (pH 5.2) were chemically modified to a total volume of 50 μl with 2.5 mM OsO_4 plus 2.5 mM 2,2′-dipyridyl disulfide for 5 min at room temperature (lanes 1–6), 2 μl DEPC for 5 min at room temperature (lanes 7–12), 2 μl 10% DMS in ethanol for 15 min at 15°C (lanes 13–18). Guanine runs are marked with roman numerals (I–VII). For DMS protection analysis, intensities of bands corresponding to guanines were measured, normalized on that of guanines outside the G-rich sequence and presented as bars in the left panel.

only cPNAs (up to 70%). Incubation with bis-PNAs led to a slight guanine modification decrease by ~30%, probably as a result of insufficient local DNA melting in the central part of the insert. Interestingly, combination of bis-PNA openers and central-binding PNAs did not result in the highest DMS protection, even with addition of telomestatin (two lower panels in Figure 6); a decrease in DMS modification was observed at the level of ~50–60%. The highest DMS protection was observed in the guanine runs II, III, V, VI and VII.

Based on these data, we believe that short PNAs binding to the complementary C-strand result in local DNA melting. This allows the G-rich strand to form G-quadruplexes in the presence of potassium ions, and this change was revealed by increased guanine N7 protection from DMS modification.

DISCUSSION

BCL2 is a potent oncogene that has a key role in apoptosis. Its overexpression is correlated with an increased chance of cancer transformation, progression and resistance to anticancer treatment. Several approaches have been explored to control *BCL2* expression, such as targeting the *BCL2* gene with triplex-forming oligonucleotides (49), antisense oligonucleotides (50) and inhibiting protein–protein interactions (51). A novel concept for gene-targeted therapy is based on the hypothesis that G-rich regions within gene promoters under certain conditions can form G-quadruplexes. Quadruplex structures could interact with transcription factors that regulate expression of these genes. Sequences with repeated guanine runs, with the potential to form quadruplexes, are overrepresented in the human genome (52). Tumor suppressor genes have very low levels of this type of sequence, while proto-oncogenes have very high levels of repeated guanine runs. G-rich regions have been found and studied in promoter regions of *PDGF* (20,21), c-*myc* (21,24), *VEGF* (21-23), *KRAS* (25) and *BCL2* (14,15).

In our study, we presented evidence for G-quadruplex formation in a second guanine-rich region of the *BCL2* gene in dsDNA. We designed a partially ds oligonucleotide with a single-stranded *BCL2* sequence overhang (*BCL2double*), and showed that this segment forms G-quadruplex structures. This was confirmed via DMS protection assay, thermal denaturing studies and CD spectrometry. The hyperchromic effect we observed was relatively weak. However, it is within the same order of magnitude as described in other quadruplex studies (48). A modest hyperchromic effect corresponds to incomplete DMS protection of guanines, which can indicate highly dynamic quadruplex formation. DMS protection was observed at the level of 60–90%, which suggests that the quadruplex structures are not entirely stable or that oligomers are switching between several types of possible G-quadruplex structures. Based solely on the CD data obtained, it is difficult to confirm the type of G-quadruplex structure observed, because there are several feasible quadruplex conformations (both intra- and inter-molecular) involving different runs of guanines in *BCL2double*. However, based on CD spectrometry, it appears a parallel quadruplex conformation predominates.

Next, we examined whether the G-rich sequence from the *BCL2* promoter region is still able to form a quadruplex after being inserted into a plasmid. We probed the plasmid with DMS, OsO_4 and DEPC, excised and labeled the G-rich strand and studied the breaks resulting from chemical modifications of the bases. The idea was to observe local DNA melting within the insert region as a result of G-quadruplex formation. KCl and telomestatin are known quadruplex stabilizing agents, but there was no sign of DNA melting within the insert; DNA remained double stranded (data shown in Supplementary Data). We inferred that the free energy provided by natural supercoiling of the plasmid was not enough to stabilize the G-quadruplex in the G-rich strand while the C-strand remains open. If G-quadruplexes do play a role in gene expression regulation in living cells, proteins that stabilize guanine quadruplexes likely bind the complementary C-rich strand selectively or in some other way interact with transcription machinery (24). For example, Duquette *et al.* (28) observed quadruplex formation during transcription. They suggested that a RNA/DNA hybrid in the C-rich strand was responsible for the guanine-rich strand release from duplex and the quadruplex formation. However, it remains unclear whether quadruplex formation actually played any role in transcription regulation or if its formation was a 'side-effect' resulting from the peculiar properties of this model. Future studies should concentrate on interactions between nuclear proteins and quadruplex forming DNA sequences to clarify the biological role of G-quadruplexes in living cells.

We sought to examine guanine quadruplex formation and stabilization utilizing short PNAs. PNAs are nucleic acid mimics in which the phosphate–sugar backbone has been replaced by *N*-(2-aminoethyl)glycine linkages (29). PNAs are resistant to degradation from proteases and nucleases and rarely interact with cellular proteins. Because PNA is uncharged, it binds to complementary DNA and RNA with higher binding affinity and selectivity than natural nucleic acids. These properties make PNA a promising tool for sequence-specific gene targeting. Another remarkable feature of PNAs is their ability to invade dsDNA, forming so-called PD loops. This phenomena was first described by Nielsen *et al.* (29,53). Later, a mechanism of invasion was proposed (54) where a triplex between one PNA and two DNA strands is formed, followed by invasion and local DNA melting. Other experiments showed higher rates of strand invasion if triplex-forming bis-homopyrimidine PNAs were used (55,56). Interestingly, PNAs invade at higher rates to targets in DNA where the displaced DNA strand can form some sort of secondary structure (cruciform) (32).

We proposed a PNA binding design (Figure 5) implementing bis-PNAs and 'central-binding PNAs' (Table 2). Our experiments show consistent PNA binding, as evidenced by the release of G-rich strands from the DNA duplex based on OsO_4 and DEPC-probing results

(Figure 6). It was shown that even with only bis-PNA openers, one can observe a noticeable degree of DNA melting in the central part of the insert. Thus, PNAs were able to bind the C-rich strand of the *BCL2* insert and release the G-rich strand. Furthermore, we observed quadruplex formation in the G-rich strand based on results from DMS protection studies. The highest rate (up to 70%) of G-quadruplex formation was observed with only central-binding PNAs. The lowest rate was ~30% with only bis-PNAs. As we have shown previously (56), binding of two bis-PNA openers did not result in the melting of the duplex region separating them. Surprisingly, the combination of central-binding PNAs and bis-PNAs led to protection from DMS at the level of 50–60%, below the level of protection afforded by cPNAs alone. We expected the combination of both types of PNA to produce the highest rates of quadruplex formation due to the greater length of the guanine-rich strand in single-stranded state. It is likely that other factors affect the ability of the released G-rich strand to form quadruplexes, such as the flexibility of the PNA/DNA complex with the C-rich strand. By analyzing DMS protection data, we cannot definitely determine which guanines within the *BCL2* segment contribute to G-quadruplex formation. Presumably, within the studied *BCL2* guanine-rich promoter sequence, there are several G-quadruplex formations involving various runs of guanines.

Recently, several groups proposed the use of G-rich quadruplex-forming PNA to target G-quadruplexes directly (34–36,57–59). In this approach, G_3 runs of PNA are involved in quadruplex formation with the G-rich strand of DNA. However, if there are proteins that specifically recognize DNA G-quadruplexes for activation or inhibition of transcription, their binding to the PNA/DNA hybrid G-quadruplex is uncertain. We designed our central-binding PNA specifically to minimize G-quadruplex formation. Although we cannot completely exclude the possibility of the quadruplex formation between central-binding PNA and the G-strand in our experiment, our goal was to extrude a native G-quadruplex in the G-rich region of the promoter to subsequently study its effect on the expression of the *BCL2* gene.

In conclusion, we induce G-quadruplex formation in the guanine-rich promoter region of the human *BCL2* gene by C-strand-invading PNAs. Our results demonstrate a new mode of sequence-specific gene targeting using short, duplex- and triplex-forming PNAs. This approach could provide a basis for future applications of gene expression regulation through G-quadruplex stabilization. In future studies, we plan to implement these PNAs for *in vivo* studies concerning regulation of the *BCL2* promoter through G-quadruplex stabilization.

SUPPLEMENTARY DATA

Supplementary Data are available at NAR Online.

ACKNOWLEDGEMENTS

We would like to thank Dr P. Schuck and Dr P. Brown for the help with CD measurements and George Leiman for critical reading of the manuscript.

FUNDING

This research was supported by the Intramural Research Program of the NIH, Clinical Center and NIDDK. Funding for open access charge: National Institutes of Health, Intramural Research Program, Clinical Center.

Conflict of interest statement. None declared.

REFERENCES

1. Akagi,T., Kondo,E. and Yoshino,T. (1994) Expression of Bcl-2 protein and Bcl-2 mRNA in normal and neoplastic lymphoid tissues. *Leuk. Lymphoma*, **13**, 81–87.
2. Joensuu,H., Pylkkanen,L. and Toikkanen,S. (1994) Bcl-2 protein expression and long-term survival in breast cancer. *Am. J. Pathol*, **145**, 1191–1198.
3. Tjalma,W., De Cuyper,E., Weyler,J., Van Marck,E., De Pooter,C., Albertyn,G. and van Dam,P. (1998) Expression of bcl-2 in invasive and in situ carcinoma of the uterine cervix. *Am. J. Obstet. Gynecol.*, **178**, 113–117.
4. Pezzella,F., Turley,H., Kuzu,I., Tungekar,M.F., Dunnill,M.S., Pierce,C.B., Harris,A., Gatter,K.C. and Mason,D.Y. (1993) bcl-2 protein in non-small-cell lung carcinoma. *N. Engl. J. Med.*, **329**, 690–694.
5. McDonnell,T.J., Troncoso,P., Brisbay,S.M., Logothetis,C., Chung,L.W., Hsieh,J.T., Tu,S.M. and Campbell,M.L. (1992) Expression of the protooncogene bcl-2 in the prostate and its association with emergence of androgen-independent prostate cancer. *Cancer Res.*, **52**, 6940–6944.
6. Chao,D.T. and Korsmeyer,S.J. (1998) BCL-2 family: regulators of cell death. *Annu. Rev. Immunol.*, **16**, 395–419.
7. Kuhlmann,T., Lucchinetti,C., Zettl,U.K., Bitsch,A., Lassmann,H. and Bruck,W. (1999) Bcl-2-expressing oligodendrocytes in multiple sclerosis lesions. *Glia*, **28**, 34–39.
8. Satou,T., Cummings,B.J. and Cotman,C.W. (1995) Immunoreactivity for Bcl-2 protein within neurons in the Alzheimer's disease brain increases with disease severity. *Brain Res.*, **697**, 35–43.
9. Marshall,K.A., Daniel,S.E., Cairns,N., Jenner,P. and Halliwell,B. (1997) Upregulation of the anti-apoptotic protein Bcl-2 may be an early event in neurodegeneration: studies on Parkinson's and incidental Lewy body disease. *Biochem. Biophys. Res. Commun.*, **240**, 84–87.
10. DeVries,A.C., Joh,H.D., Bernard,O., Hattori,K., Hurn,P.D., Traystman,R.J. and Alkayed,N.J. (2001) Social stress exacerbates stroke outcome by suppressing Bcl-2 expression. *Proc. Natl Acad. Sci. USA*, **98**, 11824–11828.
11. Seki,T., Hida,K., Tada,M., Koyanagi,I. and Iwasaki,Y. (2003) Role of the bcl-2 gene after contusive spinal cord injury in mice. *Neurosurgery*, **53**, 192–198, Discussion 198.
12. Young,R.L. and Korsmeyer,S.J. (1993) A negative regulatory element in the bcl-2 5′-untranslated region inhibits expression from an upstream promoter. *Mol. Cell Biol.*, **13**, 3686–3697.
13. Bredow,S., Juri,D.E., Cardon,K. and Tesfaigzi,Y. (2007) Identification of a novel Bcl-2 promoter region that counteracts in a p53-dependent manner the inhibitory P2 region. *Gene*, **404**, 110–116.
14. Dexheimer,T.S., Sun,D. and Hurley,L.H. (2006) Deconvoluting the structural and drug-recognition complexity of the G-quadruplex-forming region upstream of the bcl-2 P1 promoter. *J. Am. Chem. Soc.*, **128**, 5404–5415.
15. Dai,J., Chen,D., Jones,R.A., Hurley,L.H. and Yang,D. (2006) NMR solution structure of the major G-quadruplex structure

formed in the human BCL2 promoter region. *Nucleic Acids Res.*, **34**, 5133–5144.
16. Seto,M., Jaeger,U., Hockett,R.D., Graninger,W., Bennett,S., Goldman,P. and Korsmeyer,S.J. (1988) Alternative promoters and exons, somatic mutation and deregulation of the Bcl-2-Ig fusion gene in lymphoma. *EMBO J.*, **7**, 123–131.
17. Heckman,C., Mochon,E., Arcinas,M. and Boxer,L.M. (1997) The WT1 protein is a negative regulator of the normal bcl-2 allele in t(14;18) lymphomas. *J. Biol. Chem.*, **272**, 19609–19614.
18. Gomez-Manzano,C., Mitlianga,P., Fueyo,J., Lee,H.Y., Hu,M., Spurgers,K.B., Glass,T.L., Koul,D., Liu,T.J., McDonnell,T.J. *et al.* (2001) Transfer of E2F-1 to human glioma cells results in transcriptional up-regulation of Bcl-2. *Cancer Res.*, **61**, 6693–6697.
19. Huppert,J.L. and Balasubramanian,S. (2007) G-quadruplexes in promoters throughout the human genome. *Nucleic Acids Res.*, **35**, 406–413.
20. Qin,Y., Rezler,E.M., Gokhale,V., Sun,D. and Hurley,L.H. (2007) Characterization of the G-quadruplexes in the duplex nuclease hypersensitive element of the PDGF-A promoter and modulation of PDGF-A promoter activity by TMPyP4. *Nucleic Acids Res.*, **35**, 7698–7713.
21. Qin,Y. and Hurley,L.H. (2008) Structures, folding patterns, and functions of intramolecular DNA G-quadruplexes found in eukaryotic promoter regions. *Biochimie*, **90**, 1149–1171.
22. Sun,D., Guo,K., Rusche,J.J. and Hurley,L.H. (2005) Facilitation of a structural transition in the polypurine/polypyrimidine tract within the proximal promoter region of the human VEGF gene by the presence of potassium and G-quadruplex-interactive agents. *Nucleic Acids Res.*, **33**, 6070–6080.
23. Guo,K., Gokhale,V., Hurley,L.H. and Sun,D. (2008) Intramolecularly folded G-quadruplex and i-motif structures in the proximal promoter of the vascular endothelial growth factor gene. *Nucleic Acids Res.*, **36**, 4598–4608.
24. Siddiqui-Jain,A., Grand,C.L., Bearss,D.J. and Hurley,L.H. (2002) Direct evidence for a G-quadruplex in a promoter region and its targeting with a small molecule to repress c-MYC transcription. *Proc. Natl Acad. Sci. USA*, **99**, 11593–11598.
25. Cogoi,S., Paramasivam,M., Spolaore,B. and Xodo,L.E. (2008) Structural polymorphism within a regulatory element of the human KRAS promoter: formation of G4-DNA recognized by nuclear proteins. *Nucleic Acids Res.*, **36**, 3765–3780.
26. Rich,A., Nordheim,A. and Wang,A.H. (1984) The chemistry and biology of left-handed Z-DNA. *Annu. Rev. Biochem.*, **53**, 791–846.
27. Frank-Kamenetskii,M.D. and Mirkin,S.M. (1995) Triplex DNA structures. *Annu. Rev. Biochem.*, **64**, 65–95.
28. Duquette,M.L., Handa,P., Vincent,J.A., Taylor,A.F. and Maizels,N. (2004) Intracellular transcription of G-rich DNAs induces formation of G-loops, novel structures containing G4 DNA. *Genes Dev.*, **18**, 1618–1629.
29. Nielsen,P.E., Egholm,M., Berg,R.H. and Buchardt,O. (1991) Sequence-selective recognition of DNA by strand displacement with a thymine-substituted polyamide. *Science*, **254**, 1497–1500.
30. Larsen,H.J., Bentin,T. and Nielsen,P.E. (1999) Antisense properties of peptide nucleic acid. *Biochim. Biophys. Acta*, **1489**, 159–166.
31. Nielsen,P.E. and Christensen,L. (1996) Strand displacement binding of a duplex-forming homopurine PNA to a homopyrimidine duplex DNA target. *J. Am. Chem. Soc.*, **118**, 2287–2288.
32. Zhang,X., Ishihara,T. and Corey,D.R. (2000) Strand invasion by mixed base PNAs and a PNA-peptide chimera. *Nucleic Acids Res.*, **28**, 3332–3338.
33. Bukanov,N.O., Demidov,V.V., Nielsen,P.E. and Frank-Kamenetskii,M.D. (1998) PD-loop: a complex of duplex DNA with an oligonucleotide. *Proc. Natl Acad. Sci. USA*, **95**, 5516–5520.
34. Green,J.J., Ying,L., Klenerman,D. and Balasubramanian,S. (2003) Kinetics of unfolding the human telomeric DNA quadruplex using a PNA trap. *J. Am. Chem. Soc.*, **125**, 3763–3767.
35. Roy,S., Tanious,F.A., Wilson,W.D., Ly,D.H. and Armitage,B.A. (2007) High-affinity homologous peptide nucleic acid probes for targeting a quadruplex-forming sequence from a MYC promoter element. *Biochemistry*, **46**, 10433–10443.
36. Paul,A., Sengupta,P., Krishnan,Y. and Ladame,S. (2008) Combining G-quadruplex targeting motifs on a single peptide nucleic acid scaffold: a hybrid (3 + 1) PNA-DNA bimolecular quadruplex. *Chemistry*, **14**, 8682–8689.
37. He,Y., Neumann,R.D. and Panyutin,I.G. (2004) Intramolecular quadruplex conformation of human telomeric DNA assessed with 125I-radioprobing. *Nucleic Acids Res.*, **32**, 5359–5367.
38. Kutyavin,I.V., Lokhov,S.G., Afonina,I.A., Dempcy,R., Gall,A.A., Gorn,V.V., Lukhtanov,E., Metcalf,M., Mills,A., Reed,M.W. *et al.* (2002) Reduced aggregation and improved specificity of G-rich oligodeoxyribonucleotides containing pyrazolo[3,4-d]pyrimidine guanine bases. *Nucleic Acids Res.*, **30**, 4952–4959.
39. Englund,E.A. and Appella,D.H. (2007) Gamma-substituted peptide nucleic acids constructed from L-lysine are a versatile scaffold for multifunctional display. *Angew. Chem. Int. Ed. Engl.*, **46**, 1414–1418.
40. Sambrook,J., Fritsch,E.F. and Maniatis,T. (1989) *Molecular cloning: a laboratory manual*, 2nd edn. Cold Spring Harbor Laboratory Press, Cold Spring Harbor, NY.
41. Maxam,A.M. and Gilbert,W. (1980) Sequencing end-labeled DNA with base-specific chemical cleavages. *Methods Enzymol.*, **65**, 499–560.
42. Gaynutdinov,T.I., Neumann,R.D. and Panyutin,I.G. (2008) Structural polymorphism of intramolecular quadruplex of human telomeric DNA: effect of cations, quadruplex-binding drugs and flanking sequences. *Nucleic Acids Res.*, **36**, 4079–4087.
43. Rezler,E.M., Seenisamy,J., Bashyam,S., Kim,M.Y., White,E., Wilson,W.D. and Hurley,L.H. (2005) Telomestatin and diseleno sapphyrin bind selectively to two different forms of the human telomeric G-quadruplex structure. *J. Am. Chem. Soc.*, **127**, 9439–9447.
44. Giraldo,R., Suzuki,M., Chapman,L. and Rhodes,D. (1994) Promotion of parallel DNA quadruplexes by a yeast telomere binding protein: a circular dichroism study. *Proc. Natl Acad. Sci. USA*, **91**, 7658–7662.
45. Dapic,V., Abdomerovic,V., Marrington,R., Peberdy,J., Rodger,A., Trent,J.O. and Bates,P.J. (2003) Biophysical and biological properties of quadruplex oligodeoxyribonucleotides. *Nucleic Acids Res.*, **31**, 2097–2107.
46. Rujan,I.N., Meleney,J.C. and Bolton,P.H. (2005) Vertebrate telomere repeat DNAs favor external loop propeller quadruplex structures in the presence of high concentrations of potassium. *Nucleic Acids Res.*, **33**, 2022–2031.
47. Vorlickova,M., Chladkova,J., Kejnovska,I., Fialova,M. and Kypr,J. (2005) Guanine tetraplex topology of human telomere DNA is governed by the number of (TTAGGG) repeats. *Nucleic Acids Res.*, **33**, 5851–5860.
48. Mergny,J.L., Li,J., Lacroix,L., Amrane,S. and Chaires,J.B. (2005) Thermal difference spectra: a specific signature for nucleic acid structures. *Nucleic Acids Res.*, **33**, e138.
49. Shen,C., Rattat,D., Buck,A., Mehrke,G., Polat,B., Ribbert,H., Schirrmeister,H., Mahren,B., Matuschek,C. and Reske,S.N. (2003) Targeting bcl-2 by triplex-forming oligonucleotide–a promising carrier for gene-radiotherapy. *Cancer Biother. Radiopharm.*, **18**, 17–26.
50. Klasa,R.J., Gillum,A.M., Klem,R.E. and Frankel,S.R. (2002) Oblimersen Bcl-2 antisense: facilitating apoptosis in anticancer treatment. *Antisense Nucleic Acid Drug Dev.*, **12**, 193–213.
51. Oltersdorf,T., Elmore,S.W., Shoemaker,A.R., Armstrong,R.C., Augeri,D.J., Belli,B.A., Bruncko,M., Deckwerth,T.L., Dinges,J., Hajduk,P.J. *et al.* (2005) An inhibitor of Bcl-2 family proteins induces regression of solid tumours. *Nature*, **435**, 677–681.
52. Todd,A.K., Johnston,M. and Neidle,S. (2005) Highly prevalent putative quadruplex sequence motifs in human DNA. *Nucleic Acids Res.*, **33**, 2901–2907.
53. Wittung,P., Nielsen,P. and Norden,B. (1996) Direct observation of strand invasion by peptide nucleic acid (PNA) into double-stranded DNA. *J. Am. Chem. Soc.*, **118**, 7049–7054.
54. Kuhn,H., Demidov,V.V., Nielsen,P.E. and Frank-Kamenetskii,M.D. (1999) An experimental study of mechanism and specificity of peptide nucleic acid (PNA) binding to duplex DNA. *J. Mol. Biol.*, **286**, 1337–1345.
55. Griffith,M.C., Risen,L.M., Greig,M.J., Lesnik,E.A., Sprankle,K.G., Griffey,R.H., Kiely,J.S. and Freier,S.M. (1995) Single and bis peptide nucleic-acids as triplexing agents – binding and stoichiometry. *J. Am. Chem. Soc.*, **117**, 831–832.
56. Panyutin,I.G., Panyutin,I.V. and Demidov,V.V. (2007) Targeting linear duplex DNA with mixed-base peptide nucleic acid oligomers facilitated by bisPNA openers. *Anal. Biochem.*, **362**, 145–147.

57. Englund,E.A., Xu,Q., Witschi,M.A. and Appella,D.H. (2006) PNA-DNA duplexes, triplexes, and quadruplexes are stabilized with trans-cyclopentane units. *J. Am. Chem. Soc.*, **128**, 16456–16457.
58. Petraccone,L., Barone,G. and Giancola,C. (2005) Quadruplex-forming oligonucleotides as tools in anticancer therapy and aptamers design: energetic aspects. *Curr. Med. Chem. Anticancer Agents*, **5**, 463–475.
59. Amato,J., Oliviero,G., De Pauw,E. and Gabelica,V. (2009) Hybridization of short complementary PNAs to G-quadruplex forming oligonucleotides: an electrospray mass spectrometry study. *Biopolymers*, **91**, 244–255.